NASA Contractor Report 165988

NASA-CR-165988
19820018833

THE ELASTICITY PROBLEM FOR A THICK-WALLED CYLINDER CONTAINING A CIRCUMFERENTIAL CRACK

H. F. Nied and F. Erdogan

LEHIGH UNIVERSITY
Bethlehem, Pennsylvania 18015

Grant NGR 39-007-011
September 1982

National Aeronautics and
Space Administration

Langley Research Center
Hampton, Virginia 23665

THE ELASTICITY PROBLEM FOR A THICK-WALLED CYLINDER CONTAINING A CIRCUMFERENTIAL CRACK*

H.F. Nied and F. Erdogan
Lehigh University, Bethlehem, PA 18015

ABSTRACT

The elasticity problem for a long hollow circular cylinder containing an axisymmetric circumferential crack subjected to general nonaxisymmetric external loads is considered. The problem is formulated in terms of a system of singular integral equations with the Fourier coefficients of the derivative of the crack surface displacement as density functions. The stress intensity factors and the crack opening displacement are calculated for a cylinder under uniform tension, bending by end couples, and self-equilibrating residual stresses.

1. Introduction

The elasticity problem for a cylindrical structure such as a pressure vessel or a pipe which contains a part-through surface crack appears to be analytically intractable. Such problems are generally treated either numerically by using the technique of the finite elements [1,2] or the boundary integral equations [3], or, in relatively thin-walled cylinders, approximately by using the line spring model in conjunction with the shell theory [4,5]. The limiting cases of some of these problems can also be solved analytically which provide very useful results, for example, regarding the bounds of stress intensity factors. The plane strain problem of a hollow cylinder containing a crack in a radial plane which constitutes the limiting case of a cylinder with an axial part-through crack is one such problem. Another problem is that of a long thick-walled cylinder which contains an axisymmetric radial crack. In this paper the latter

(*) This work was supported by NSF under the Grant CME-78-09737, by NASA-Langley under the Grant NGR 39-007-011 and by DOT under the contract DOT-RC-82007.

problem is considered for arbitrary nonaxisymmetric loading conditions. The related problem for an elastic solid cylinder containing a penny-shaped crack is considered in [6-8], and that for a hollow cylinder under axisymmetric loading conditions in [9].

2. Formulation of the Problem

The problem under consideration is described in Fig. 1. The external loads may be decomposed in such a way that the problem may be expressed as the superposition of a problem which is symmetric and that which is anti-symmetric with respect to the z=0 plane. In this paper, only the symmetric problem is treated. Clearly, it is sufficient to consider one half (e.g., z>0) of the medium only. Furthermore, for the given external loads the quasistatic problem for the cylinder without the crack is assumed to have been solved. Thus, the information regarding the stress intensity factors may be obtained by considering the perturbation problem in which the crack surface tractions are the only external loads. Following are then the boundary and continuity conditions of the problem:

$$\sigma_{rr}(a,\theta,z) = \tau_{rz}(a,\theta,z) = \tau_{r\theta}(a,\theta,z) = 0,\ 0\leq\theta\leq 2\pi,\ 0\leq z<\infty\ , \tag{1}$$

$$\sigma_{rr}(b,\theta,z) = \tau_{rz}(b,\theta,z) = \tau_{r\theta}(b,\theta,z) = 0,\ 0\leq\theta\leq 2\pi,\ 0\leq\theta\leq 2\pi, \tag{2}$$

$$\tau_{zr}(r,\theta,0) = \tau_{z\theta}(r,\theta,0) = 0,\ a\leq r\leq b,\ \ 0\leq\theta\leq 2\pi\ , \tag{3}$$

$$\sigma_{zz}(r,\theta,0) = p(r,\theta)\ ,\ c<r<d\ ,\ 0\leq\theta\leq 2\pi\ , \tag{4a}$$

$$u_z(r,\theta,0) = 0,\ a\leq r<c,\ d<r\leq b,\ 0\leq\theta\leq 2\pi\ , \tag{4b}$$

where the dimensions of the cylinder and the crack are given in Fig. 1 and $p(r,\theta)$ is a known function. Also, the stresses must vanish as $z\to\infty$.

Referring to [10], [11], and [8] the solution of the problem may be expressed in terms of a system of five harmonic functions as follows:

$$2\mu u_r = (1-2\nu)\frac{\partial \phi}{\partial r} + z\frac{\partial^2 \phi}{\partial r \partial z} + 2\mu u_{r2} \tag{5}$$

$$2\mu u_\theta = (1-2\nu)\frac{1}{r}\frac{\partial \phi}{\partial \theta} + \frac{z}{r}\frac{\partial^2 \phi}{\partial \theta \partial z} + 2\mu u_{\theta 2} \tag{6}$$

$$2\mu u_z = -2(1-\nu)\frac{\partial \phi}{\partial z} + z\frac{\partial^2 \phi}{\partial z^2} + 2\mu u_{z2} \tag{7}$$

$$\sigma_{rr} = z\frac{\partial^3 \phi}{\partial r^2 \partial z} + \frac{\partial^2 \phi}{\partial r^2} - 2\nu\left(\frac{\partial^2 \phi}{\partial r^2} + \frac{\partial^2 \phi}{\partial z^2}\right) + 2\mu\left(\frac{\nu\Delta}{1-2\nu} + \frac{\partial u_{r2}}{\partial r}\right), \tag{8}$$

$$\sigma_{\theta\theta} = -(1-2\nu)\frac{\partial^2 \phi}{\partial r^2} + \frac{z}{r^2}\frac{\partial^3 \phi}{\partial \theta^2 \partial z} + \frac{z}{r}\frac{\partial^2 \phi}{\partial r \partial z} - \frac{\partial^2 \phi}{\partial z^2}$$

$$+ 2\mu\left[\frac{\nu\Delta}{1-2\nu} + \frac{1}{r}\left(\frac{\partial u_{\theta 2}}{\partial \theta} + u_{r2}\right)\right] \tag{9}$$

$$\sigma_{zz} = z\frac{\partial^3 \phi}{\partial z^3} - \frac{\partial^2 \phi}{\partial z^2} + 2\mu\left(\frac{\nu\Delta}{1-2\nu} + \frac{\partial u_{z2}}{\partial z}\right), \tag{10}$$

$$\tau_{zr} = z\frac{\partial^3 \phi}{\partial r \partial z^2} + \mu\left(\frac{\partial u_{r2}}{\partial z} + \frac{\partial u_{z2}}{\partial r}\right), \tag{11}$$

$$\tau_{z\theta} = \frac{z}{r}\frac{\partial^3 \phi}{\partial \theta \partial z^2} + \mu\left(\frac{1}{r}\frac{\partial u_{z2}}{\partial \theta} + \frac{\partial u_{\theta 2}}{\partial z}\right), \tag{12}$$

$$\tau_{r\theta} = (1-2\nu)\left(\frac{1}{r}\frac{\partial^2 \phi}{\partial r \partial \theta} - \frac{1}{r^2}\frac{\partial \phi}{\partial \theta}\right) - \frac{z}{r^2}\frac{\partial^2 \phi}{\partial \phi \partial z} + \frac{z}{r}\frac{\partial^3 \phi}{\partial r \partial \theta \partial z}$$

$$+ \mu\left(\frac{1}{r}\frac{\partial u_{r2}}{\partial \theta} + \frac{\partial u_{\theta 2}}{\partial r} - \frac{u_{\theta 2}}{r}\right), \tag{13}$$

where

$$\Delta = \frac{\partial u_{r2}}{\partial r} + \frac{u_{r2}}{r} + \frac{1}{r}\frac{\partial u_{\theta 2}}{\partial \theta} + \frac{\partial u_{z2}}{\partial z}, \tag{14}$$

$$2\mu u_{r2} = (3-4\nu)[B_1\cos\theta + B_2\sin\theta] - r[\frac{\partial B_1}{\partial r}\cos\theta + \frac{\partial B_2}{\partial r}\sin\theta] - \frac{\partial B_0}{\partial r} + \frac{2}{r}\frac{\partial \psi}{\partial \theta} \tag{15}$$

$$2\mu u_{\theta 2} = (3-4\nu)[B_2\cos\theta - B_1\sin\theta] - [\frac{\partial B_1}{\partial \theta}\cos\theta + \frac{\partial B_2}{\partial \theta}\sin\theta] - \frac{1}{r}\frac{\partial B_0}{\partial \theta} - 2\frac{\partial \psi}{\partial r} \tag{16}$$

$$2\mu u_{z2} = -r\frac{\partial B_1}{\partial z}\cos\theta - r\frac{\partial B_2}{\partial z}\sin\theta - \frac{\partial B_0}{\partial z} \tag{17}$$

The harmonic function ϕ is associated with the formulation of the problem for an infinite elastic space for which z=0 is a plane of symmetry [10]. The functions B_0, B_1, B_2 and ψ are equivalent to Papkovich-Neuber potentials in cylindrical coordinates [11,8]. With an important application of the bending of the cylinder in mind, if we restrict the considerations to external loads which are symmetric in θ, that is, if $p(r,\theta) = p(r,-\theta)$, then the functions p and ϕ may be expressed as

$$p(r,\theta) = \sum_0^\infty \sigma_n(r)\cos n\theta\ , \tag{18}$$

$$\phi(r,\theta,z) = \sum_0^\infty \cos n\theta \int_0^\infty A_n(\alpha)J_n(\alpha r)\alpha e^{-\alpha z}\, d\alpha, \tag{19}$$

where the functions A_n, (n=0,1,...) are unknown and

$$\sigma_0(r) = \frac{1}{\pi}\int_0^\pi p(r,\theta)d\theta,\ \sigma_n(r) = \frac{2}{\pi}\int_0^\pi p(r,\theta)\cos n\theta d\theta,\ (n=1,2,...)\ . \tag{20}$$

For the symmetric loading under consideration from (5)-(17) it may be seen that B_0 and B_1 are even and B_2 and ψ are odd in θ. Taking also into account the symmetry with respect to the z=0 plane, these harmonic functions may be written in the following form:

$$B_1 = \sum_{n=0}^{\infty} \cos[(n+1)\theta] \frac{2}{\pi} \int_0^{\infty} [C_{1n}(s)I_{n+1}(sr) + C_{2n}(s)K_{n+1}(sr)]\cos(sz)ds, \tag{21}$$

$$B_2 = \sum_{n=0}^{\infty} \sin[(n+1)\theta] \frac{2}{\pi} \int_0^{\infty} [C_{1n}(s)I_{n+1}(sr)+C_{2n}(s)K_{n+1}(sr)]\cos(sz)ds , \tag{22}$$

$$B_0 = \sum_{n=0}^{\infty} \cos(n\theta) \frac{2}{\pi} \int_0^{\infty} [C_{3n}(s)I_n(sr)+C_{4n}(s)K_n(sr)]\cos(sz)ds , \tag{23}$$

$$\psi = \sum_{n=0}^{\infty} \sin(n\theta) \frac{2}{\pi} \int_0^{\infty} [C_{5n}(s)I_n(sr)+C_{6n}(s)K_n(sr)]\cos(sz)ds . \tag{24}$$

where I_n and K_n are modified Bessel functions and the functions C_{in}, $(i=1,\ldots,6;\ n=0,1,\ldots)$ are as yet unknown.

From the formulation of the problem as stated, it may be verified that the conditions (3) are identically satisfied. The seven sets of unknown functions A_n, $C_{1n},\ldots, C_{6n}$, $n=0,1,\ldots$ are then obtained from the seven conditions (1), (2), and (4) by observing that these conditions are in the form of sine or cosine series, and hence, by writing the coefficients of $\sin n\theta$ or $\cos n\theta$ equal to zero for each n. Thus, for each n the homogeneous conditions (1) and (2) are used to eliminate six of the unknowns and the mixed boundary condition (4) is used to determine the remaining unknown function. The integral equation of the problem may be obtained directly by expressing

$$u_z(r,\theta,0) = \sum_{0}^{\infty} \phi_n(r)\cos n\theta, \quad a\leq r\leq b, \quad 0\leq\theta\leq 2\pi, \tag{25}$$

where from (4b) it follows that

$$\phi_n(r) = 0, \quad a\leq r<c, \quad d<r\leq b, \quad (n=0,1,\ldots) \tag{26}$$

From (7), (19) and (21)-(26) it follows that

$$A_n(\alpha) = \frac{\mu}{1-\nu}\frac{1}{\alpha}\int_c^d \phi_n(t)J_n(\alpha t)tdt \ . \tag{27}$$

By using the conditions (1) and (2), the unknown functions $C_{1n},\ldots,$ C_{6n} may be obtained in terms of ϕ_n in the following form:

$$C_{in}(s) = -\frac{\mu}{1-\nu}\sum_{j=1}^{6} m_{ij}(s)\int_c^d t\phi_n(t)G_j(s,t)dt, \ (i=1,\ldots,6;\ n=0,1,\ldots) \tag{28}$$

where the functions m_{ij} and G_j, $(i,j=1,\ldots,6)$ are given in Appendix A. Finally, from (4a) and (18), it follows that

$$\lim_{z\to 0}\Big[\int_0^\infty -(1+\alpha z)A_n(\alpha)J_n(\alpha r)\ \alpha^3 e^{-\alpha z}\ d\alpha$$

$$+\frac{2}{\pi}\int_0^\infty s\sum_{i=1}^{4} C_{in}(s)N_i(r,s)ds = \sigma_n(r),\ (n=0,1,\ldots)\ , \tag{29}$$

where

$$N_1 = 2\nu I_n(sr) + sr\ I_{n+1}(sr),\ N_2 = -2\nu\ K_n(sr) + sr\ K_{n+1}(sr),$$

$$N_3 = s\ I_n(sr),\ N_4 = s\ K_n(sr)\ . \tag{30}$$

Substituting now from (27) into (29), through an asymptotic analysis separating the singular part of the kernel, and by integrating by parts we obtain

$$[\phi_n(t)\{-\frac{1}{\pi}(\frac{t}{r})^{\frac{1}{2}}\frac{1}{t-r} - L_1(t,r) - L_2(t,r)\}]_{t=c}^{t=d}$$

$$+\int_c^d [\frac{1}{\pi}(\frac{t}{r})^{\frac{1}{2}}\frac{1}{t-r} + L_1(t,r) + L_2(t,r)]\phi_n'(t)\,dt$$

$$= \frac{1-\nu}{\mu}\sigma_n(r),\ c<r<d,\ n=0,1,\ldots \tag{31}$$

where the kernels L_1 and L_2 are given by

$$L_1(t,r) = -\frac{1}{\pi}\frac{1}{2r}\log\left[\frac{(t^{\frac{1}{2}}-r^{\frac{1}{2}})^2}{|t-r|}\right] + \int_0^\infty \{\alpha t[n\,J_n(\alpha t)S_{0,n-1}(\alpha t)$$

$$- J_{n-1}(\alpha t)S_{1,n}(\alpha t)]J_n(\alpha r) - \frac{1}{\pi}\frac{\sqrt{t}}{r}[\sin\alpha(t-r) - (1)^n\cos\alpha(t+r)]$$

$$- \frac{1}{\sqrt{2\pi r\alpha}}[C(\sqrt{\alpha t})(\sin(\alpha r)+(-1)^n\cos(\alpha r)) - S(\sqrt{\alpha t})(\cos(\alpha r)$$

$$+ (-1)^n \sin(\alpha r))]\}d\alpha\ . \tag{32}$$

$$L_2(t,r) = \frac{2}{\pi}\int_0^\infty \sum_{i=1}^{4}\sum_{j=1}^{6} m_{ij}(s)N_i(s,r)v_j(s,t)s\,ds. \tag{33}$$

The function $S_{\mu,\nu}(z)$ which appears in (29) is the Lommel's function [12,13], and $C(x)$ and $S(x)$ are the Fresnel integrals defined by [14]

$$C(x) = \frac{1}{\sqrt{2\pi}}\int_0^{x^2}\frac{\cos t}{\sqrt{t}}\,dt\ ,\ S(x) = \frac{1}{\sqrt{2\pi}}\int_0^{x^2}\frac{\sin t}{\sqrt{t}}\,dt\ . \tag{34}$$

The functions $v_j(s,t)$ appearing in (33) are given in Appendix B. A convenient numerical technique for the evaluation of Lommel's functions of real and imaginary arguments is described in Appendices C and B.

The infinite integrals which appear in (32) converge rather slowly for nearly all values of r and t. The reason for this is that, considered term by term, all integrals in (32) are divergent. However, it can be shown that the asymptotic behavior of the terms for large values of α is identical but opposite in sign to the trigonometric terms in the integrand and the sum leads to a convergent integral. The realted asymptotic analysis and the numerical evaluation of these integrals are described in Appendix D.

3. The Stress Intensity Factors

The Mode I stress intensity factors along the crack borders r=c and r=d are defined by

$$k(c) = \lim_{r\to c} \sqrt{2(c-r)}\, \sigma_{zz}(r,\theta,0) \ , \tag{35}$$

$$k(d) = \lim_{r\to d} \sqrt{2(r-d)}\, \sigma_{zz}(r,\theta,0) \ , \tag{36}$$

and, in terms of the crack surface displacement, may be expressed as

$$k(c) = \frac{\mu}{1-\nu} \lim_{r\to c} \sqrt{2(r-c)}\, \frac{\partial}{\partial r} u_z(r,\theta,0)$$

$$= \frac{\mu}{1-\nu} \lim_{r\to c} \sqrt{2(r-c)} \sum_{o}^{\infty} \phi_n'(r) \cos n\theta \tag{37}$$

$$k(d) = -\frac{\mu}{1-\nu} \lim_{r\to d} \sqrt{2(d-r)}\, \frac{\partial}{\partial r} u_z(r,\theta,0)$$

$$= -\frac{\mu}{1-\nu} \lim_{r\to d} \sqrt{2(d-r)} \sum_{o}^{\infty} \phi_n'(r) \cos n\theta \ . \tag{38}$$

The formulation given in the previous section is valid provided the external load $p(r,\theta)$ is such that the crack surface displacement $u_z(r,\theta,0)$ is positive everywhere in $(c<r<d,\ 0\le\theta\le 2\pi)$. In this case, the stress intensity factors k(c) and k(d) would be positive for all values of θ.

4. The Embedded Crack

Referring to Fig. 1, if c>a and d<b the crack is embedded and the crack surface displacement is zero at r=c and r=d. From (25) it then follows that $\phi_n(c) = 0 = \phi_n(d)$, the integrated terms on the left-hand side of the integral equation (31) vanish and the integral equations must be solved under the following conditions (see (26):

$$\int_c^d \phi_n'(t)dt = 0 , \quad n = 0,1,... \tag{39}$$

The solution of the singular integral equation (31) is of the form

$$\phi_n'(t) = f_n(t)[(t-c)(d-t)]^{-\frac{1}{2}} , \quad c < t < d , \tag{40}$$

where $f_n(t)$ is a bounded function. After normalizing the interval (c,d) by defining

$$t = \frac{d-c}{2}\tau + \frac{d+c}{2} , \quad r = \frac{d-c}{2}\rho + \frac{d+c}{2} , \quad f_n(t) = F_n(\tau), \tag{41}$$

The functions $F_n(\tau)$, n=0,1,... may be obtained from (31) by using a Gauss-Chebyshev type quadrature formula [15].

5. The Edge Cracks

If the crack is a surface or an edge crack, then the crack surface displacement will be zero only at one tip and consequently the conditions (39) will no longer be valid. In this case (the Fourier coefficients of) the crack opening displacement on the cylinder surface may be expressed as

$$a = c < d < b: \quad \phi_n(d) = 0 , \quad \phi_n(c) = -\int_c^d \phi_n'(t)dt , \tag{42}$$

$$a < c < d = b: \quad \phi_n(c) = 0 , \quad \phi_n(d) = \int_c^d \phi_n'(t)dt , \tag{43}$$

for the inner and the outer edge cracks, respectively. For these crack configurations, even though the integral equation (31) is still valid, the integrated terms on the left-hand side are not zero and by using (42) and (43), (31) may be expressed as

$$\int_c^d \{\frac{1}{\pi}\left[\left(\frac{t}{r}\right)^{\frac{1}{2}}\frac{1}{t-r} - \left(\frac{s}{r}\right)^{\frac{1}{2}}\frac{1}{s-r}\right] + L_1(t,r) - L_1(s,r)$$

$$+ L_2(t,r)-L_2(s,r)\}\phi'(t)dt = \frac{1-\nu}{\mu}\sigma_n(r),\ c<r<d,\ n=0,1,\ldots \qquad (44)$$

where $s = c = a<d<b$ for the internal edge crack and $s = d = b>c>a$ for the external edge crack.

For the edge cracks even though the kernel $L_2(t,r)$ contains additional singular terms (in the form of generalized Cauchy singularities) which become unbounded as t and r go to the end point s simultaneously, as seen from (44) for $(t,r) \to s$ the entire kernel in (44) vanishes. As shown in [16], the consequence of this is that the derivative of the crack surface displacement at r=s (i.e., on the cylinder surface) is bounded. This point is rather important in the numerical solution of the integral equation. For the embedded crack, in the Gaussian integration, referring to (41) the unknowns and the collocation points are $F_n(\tau_i)$ and ρ_j, respectively where

$$\tau_i = \cos\left(\pi\frac{i-1}{m-1}\right),\ i = 1,\ldots,m\ , \qquad (45)$$

$$\rho_j = \cos\left(\pi\frac{2j-1}{2m-2}\right),\ j = 1,\ldots,m-1\ . \qquad (46)$$

The additional equation to solve for m unknowns $F_n(\tau_i)$, $(i=1,\ldots,m)$ is provided by (39). However, in the edge crack problem (39) is not valid and consequently there are only m-1 algebraic equations. In this case since the column in the coefficient matrix obtained from (44) which corresponds to t=s, i.e., $\tau=1$ or $\tau=-1$, is identically zero, the system of algebraic equations involve m-1 unknowns only and hence gives a unique solution.

After obtaining ϕ_n' the stress intensity factor at the crack tip may again be obtained by using (37) or (38). In the edge crack problem another quantity of some interest is the crack opening displacement at the cylinder surface which, referring to (25), (42), and (43), may be obtained from

$$\delta = u_z(a,\theta,+0) - u_z(a,\theta,-0) = -2\sum_{o}^{\infty} \cos n\theta \int_a^d \phi_n'(t)dt \ , \tag{46}$$

$$\delta = u_z(b,\theta,+0) - u_z(b,\theta,-0) = 2\sum_{o}^{\infty} \cos n\theta \int_c^b \phi_n'(t)dt \ . \tag{47}$$

6. Results

The numerical results given in this section are obtained for three different loading conditions, namely the uniform axial stress, the bending of the cylinder by end couples, and the self-equilibrating residual stress. For these three loading conditions the crack surface tractions in the perturbation problem are respectively given by (see (4a) and (18))

$$p(r,\theta) = \sigma_o(r) = -\sigma_o = -\frac{P_\infty}{\pi(b^2-a^2)} \ , \tag{48}$$

$$p(r,\theta) = \sigma_1(r)\cos\theta = -\sigma_1\left(\frac{r}{b}\right)\cos\theta \ , \ \sigma_1 = \frac{4Mb}{\pi(b^4-a^4)}, \tag{49}$$

$$p(r,\theta) = \sigma_o(r) = -\sigma_s \left[\frac{6(r-a)(b-r)}{(b-a)^2} - 1\right] \ , \tag{50}$$

where P_∞ is the axial force, M is the bending moment, and σ_s is the magnitude of the compressive stress on the surfaces of the cylinder. In the residual stress problem the axial stress $\sigma_z(r,\theta,0)$ is assumed to be independent of θ, parabolic in r, compressive on and near the surfaces, tensile in the interior region of the cylinder wall, and statically self-equilibrating. Unless otherwise stated, in all examples the Poisson's ratio is assumed to be 0.3.

For a ring-shaped crack in an infinite solid (i.e., for a=0, b=∞) the calculated stress intensity factors are shown in Figure 2. Here σ_0 is the uniform crack surface pressure, for n=1 the crack surface traction is defined by

$$p(r,\theta) = \sigma_1(r)\cos\theta = -\sigma_1 \left(\frac{r}{d}\right)\cos\theta \ , \tag{51}$$

and

$$k = k(s,\theta) = k'(s)_n \ \sigma_n\left(\frac{d-c}{2}\right)^{\frac{1}{2}} \cos n\theta \ , \ (n=0,1) \tag{52}$$

is the stress intensity factor along the crack edges s=c and s=d. Note that as c/d approaches 1 and 0, respectively, the plane strain and the penny-shaped crack results are recovered.

For hollow cylinders under tension or bending the results are given in Tables 1-17. Tables 1-3 show the stress intensity factors for a symmetrically located imbedded crack (i.e., for b-d = c-a, Figure 1). Here the normalizing stresses σ_0 and σ_1 are defined by (48) and (49). As (a/b) → 1 the curvature effect disappears and the stress intensity factors approach those obtained from the plane strain solution of a strip containing a center crack.

Tables 4-15 show the stress intensity factors and the crack opening displacements for an internal or an external surface crack. Here ℓ is the total crack depth (ℓ = d-a for c = a and ℓ = b-c for d=b), h = b-a is the wall thickness (Figure 1), and the crack opening displacement δ is defined by (46) and (47). For a very small crack depth (i.e., for $\ell/h = 0.01$) the effect of a/b on k is shown in Figure 3. In this case the stress intensity factors for a half plane, for a strip and for a solid cylinder are practically the same (i.e., $k/\sigma_0\sqrt{\ell} \cong 1.121$). It is seen that for the internal edge crack as a/b approaches 0 and 1 $k/\sigma_0\sqrt{\ell}$ approaches respectively $2/\pi$ and 1.121 which are the values for a penny-shaped crack and for a strip. For the external edge crack, on the other hand the influence of a/b on k is hardly noticeable.

The limiting values of k and δ for (a/b) → 1 shown in the tables are obtained from the plane strain solution of a strip containing an

edge crack. The stress intensity factor for an internal edge crack seems to be a monotonously increasing function of a/b for all crack depths. On the other hand, for an external edge crack k always seems to go through a minimum as a/b goes from 0 to 1.

For one crack-cylinder geometry, namely for a=c<d<b, (a/b) = 0.5 and (ℓ/h) = 0.3 the effect of Poisson's ratio on k and δ is shown in Tables 16 and 17. It may be seen that both k and δ increase monotonously but very slightly with increasing Poisson's ratio.

For the residual stress problem the crack geometry and the stress profile are shown in Figure 4. It is clear that if the crack is sufficiently shallow so that it lies in the compressive zones near the surfaces, then the crack surfaces would remain closed and k would be zero. In the example under consideration by letting $\sigma_0(r_i) = 0$ (i = 1,2) in (50) we find

$$\frac{r_1-a}{b-a} = 0.211 \quad , \quad \frac{r_2-a}{b-a} = 0.789 \tag{53}$$

where $r_1<r<r_2$ is the tensile region. If r_0 defines the crack tip as shown in Figure 4, for $r_0>r_1$ in the inner edge crack and for $r_0<r_2$ in the outer edge crack case the crack tip will be in the tensile zone of the cylinder and k will be positive. However, in this case the crack surfaces will still be partially closed and, hence, the problem is a crack-contact problem with the depth ε of the contact zone being an unknown constant. The physical condition which accounts for this unknown is the smooth closure condition of the crack surfaces at r=a+ε or r=b-ε. Thus, the problem may now be treated as an embedded crack problem with the crack surface traction p as given by (50) and c=a+ε, d=r_0, ($r_0>r_1$) for inner edge crack, and c=r_0, ($r_0<r_2$), d=b-ε for outer edge crack case. In each case, the smooth closure condition to account for the unknown constant ε may then be expressed as

$$k(a+\varepsilon) = 0 \quad , \quad k(b-\varepsilon) = 0 \quad . \tag{54}$$

For two cylinders with thickness ratios a/b = 0.7 and 0.9, Figure 5 shows the stress intensity factor $k(r_0)$. Note that k is positive for

$r_1 < r_0 < b$ in the inner edge crack case and for $a < r_0 < r_2$ in the outer edge crack case where r_1 and r_2 are given by (53). Also note that initially as the crack length ℓ increases (Figure 4) k increases, goes through a maximum and tends to zero as the crack traverses the entire cylinder wall. Similar results have been observed for flat plates [18].

For a/b = 0.9 the length ε of the contact region is shown in Figure 6. For example, in the case of the internal edge crack $\varepsilon = \ell$, that is the crack is fully closed for $\ell \leq r_1 - a$ where $(r_1 - a)/(b - a) = 0.211$. For $\ell > r_1 - a$, ε decreases monotonously and tends to zero (asymptotically) as $\ell \to b - a$.

References

1. Newman, J.C., and Raju, I.S., "Stress Intensity Factors for Internal Surface Cracks in Cylindrical Pressure Vessels", NASA Technical Memorandum 80073, July 1979.

2. McGowan, J.J. and Raymund, M., "Stress Intensity Factor Solutions for Internal Longitudinal Semi-Elliptic Surface Flaws in a Cylinder under Arbitrary Loadings", Fracture Mechanics, ASTM-STP 677, 1979.

3. Heliot, J., Labbens, R.C., and Pellisier-Tanon, A., "Semi-Elliptic Cracks in a Cylinder Subjected to Stress Gradients", Fracture Mechanics, ASTM-STP 677, 1979.

4. Parks, D.M., "The Inelastic Line-Spring: Estimates of Elastic Plastic Fracture Mechanics Parameters for Surface-Cracked Plates and Shells", Paper 80-C2/PVP-109, ASME, 1980.

5. Delale, F. and Erdogan, F., "Application of the Line-Spring Model to a Cylindrical Shell Containing a Circumferential or Axial Part-Through Crack", to appear in J. Appl. Mech., Trans. ASME, 1982.

6. Sneddon, I.N. and Tait, J.T., "The Effect of a Penny-shaped Crack on the Distribution of Stress in a Long Circular Cylinder", Int. J. Engng. Sci., Vol. 1, pp. 391-409, 1963.

7. Sneddon, I.N. and Welch, J.T., "A Note on the Distribution of Stress in a Cylinder Containing a Penny-shaped Crack", Int. J. Engng. Sci., Vol. 1, pp. 411-419, 1963.

8. Kassir, M.K. and Singh, M., "Non-Axisymmetric Loadings of a Crack Cylinder", Int. J. Solids Structures, Vol. 14, pp. 153-160, 1978.

9. Erdol, R. and Erdogan, F., "A Thick-walled Cylinder with an Axisymmetric Internal or Edge Crack", J. Appl. Mech., Vol. 45, Trans. ASME, pp. 281-286, 1978.

10. Green, A.E. and Zerna, W., Theoretical Elasticity, Oxford University Press, London, 1968.

11. Lurė, A.I., Three-Dimensional Problems of the Theory of Elasticity, Interscience Publishers, 1964.

12. Magnus, W., Oberhettinger, F., Soni, R.P., Formulas and Theorems for the Special Functions of Mathematical Physics, Die Grundlehren der mathematischen Wissenschaften, Vol. 52, Springer-Verlag, New York, 1966.

13. Watson, G.N., A Treatise on the Theory of Bessel Functions, 2nd ed., Cambridge University Press, London, 1944.

14. Gradshteyn, I.S. and Ryzhik, I.M., Tables of Integrals, Series and Products, 4th ed., Academic Press, New York, 1966.

15. Erdogan, F., "Mixed Boundary Value Problems in Mechanics", Mechanics Today, Nemat-Nasses, S., ed., Vol. 4, pp. 1-86, Pergamon Press, Oxford, 1978.

16. Gupta, G.D. and Erdogan, F., "The Problem of Edge Cracks in an Infinite Strip", J. Appl. Mech., Vol. 41, Trans. ASME, pp. 1001-1006, 1974.

17. Erdélyi, A., ed., Table of Integral Transforms - Bateman Manuscript Project, Vol. 2, McGraw-Hill, New York, 1954.

18. Bakioglu, M., Erdogan, F., and Hasselman, D.H.P., "Fracture Mechanical Analysis of Self-Fatigue in Surface Compression Strengthened Glass Plates", J. Material Science, Vol. 11, pp. 1826-1834, 1976.

19. Nied, H.F., "Circumferentially Cracked Cylinders under Extension or Bending", Ph.D. Dissertation, Lehigh University, 1981.

Table 1. Stress intensity factors for a symmetric embedded crack in a thick-walled cylinder subjected to axial tension and pure bending. $((d-c)/(b-a)=0.1$, $\sigma_0 = P_\infty/[\pi(b^2-a^2)]$, $\sigma_1=4Mb/[\pi(b^4-a^4)])$.

$\frac{a}{b}$	$\frac{d-c}{b}$	$\frac{c}{b}$	$\frac{k(c)}{\sigma_0\sqrt{\frac{d-c}{2}}}$	$\frac{k(d)}{\sigma_0\sqrt{\frac{d-c}{2}}}$	$\frac{k(c)}{\sigma_1\sqrt{\frac{d-c}{2}}\cos\theta}$	$\frac{k(d)}{\sigma_1\sqrt{\frac{d-c}{2}}\cos\theta}$
0.1	0.09	0.505	1.028	0.989	0.538	0.562
0.2	0.08	0.56	1.024	0.991	0.590	0.612
0.3	0.07	0.615	1.020	0.994	0.643	0.662
0.4	0.06	0.67	1.017	0.996	0.695	0.711
0.5	0.05	0.725	1.014	0.998	0.747	0.761
0.6	0.04	0.78	1.012	1.000	0.799	0.810
0.7	0.03	0.835	1.010	1.002	0.851	0.859
0.8	0.02	0.89	1.009	1.003	0.903	0.908
0.9	0.01	0.945	1.007	1.005	0.954	0.957
→1.0	→0	→1	→1.006	→1.006	→1.006	→1.006

Table 2. Stress intensity factors for a symmetric embedded crack in a thick-walled cylinder subjected to axial tension and pure bending. $((d-c)/(b-a)=0.5$, $\sigma_0 = P_\infty/[\pi(b^2-a^2)]$, $\sigma_1=4Mb/[\pi(b^4-a^4)])$.

$\frac{a}{b}$	$\frac{d-c}{b}$	$\frac{c}{b}$	$\frac{k(c)}{\sigma_0\sqrt{\frac{d-c}{2}}}$	$\frac{k(d)}{\sigma_0\sqrt{\frac{d-c}{2}}}$	$\frac{k(c)}{\sigma_1\sqrt{\frac{d-c}{2}}\cos\theta}$	$\frac{k(d)}{\sigma_1\sqrt{\frac{d-c}{2}}\cos\theta}$
0.1	0.45	0.325	1.383	1.117	0.506	0.671
0.2	0.40	0.40	1.330	1.124	0.593	0.733
0.3	0.35	0.475	1.294	1.131	0.677	0.795
0.4	0.30	0.55	1.268	1.139	0.758	0.856
0.5	0.25	0.625	1.247	1.147	0.836	0.914
0.6	0.20	0.70	1.231	1.155	0.911	0.971
0.7	0.15	0.775	1.217	1.162	0.984	1.026
0.8	0.10	0.85	1.206	1.170	1.054	1.080
0.9	0.05	0.925	1.196	1.178	1.121	1.133
→1.0	→0	→1	→1.187	→1.187	→1.187	→1.187

Table 3. Stress intensity factors for a symmetric embedded crack in a thick-walled cylinder subjected to axial tension. $((d-c)/(b-a)=0.9,\ \sigma_0=P_\infty/[\pi(b^4-a^4)])$.

$\frac{a}{b}$	$\frac{d-c}{b}$	$\frac{c}{b}$	$\frac{k(c)}{\sigma_0 \frac{d-c}{2}}$	$\frac{k(d)}{\sigma_0 \frac{d-c}{2}}$
0.1	0.81	0.145	3.740	2.412
0.2	0.72	0.24	3.300	2.404
0.3	0.63	0.335	3.081	2.410
0.4	0.54	0.43	2.945	2.422
0.5	0.45	0.525	2.850	2.437
0.6	0.36	0.62	2.778	2.456
0.7	0.27	0.715	2.720	2.479
0.8	0.18	0.81	2.671	2.506
0.9	0.09	0.905	2.627	2.536
→1.0	→0	→1	→2.585	→2.585

Table 4. Stress intensity factors and crack opening displacements for an internal edge crack in a thick-walled cylinder subjected to axial tension and pure bending. $(\ell/h=0.1,\ h=b-a,\ \sigma_0=P_\infty/[\pi(b^2-a^2)],\ \sigma_1=4Mb/[\pi(b^4-a^4)])$.

$\frac{a}{b}$	$\frac{k(d)}{\sigma_0\sqrt{\ell}}$	$\frac{k(d)}{\sigma_1\sqrt{\ell}\cos\theta}$	$\frac{\mu}{1-\nu}\frac{\delta(c)}{h\,\sigma_0}$	$\frac{\mu}{1-\nu}\frac{\delta(c)}{h\sigma_1\cos\theta}$
0	0.637	0.042	0.128	0
0.1	0.842	0.123	0.212	0.021
0.2	0.940	0.225	0.244	0.050
0.3	1.000	0.334	0.261	0.080
0.4	1.042	0.447	0.272	0.111
0.5	1.073	0.563	0.281	0.142
0.6	1.097	0.680	0.287	0.174
0.7	1.119	0.800	0.292	0.206
0.8	1.138	0.922	0.297	0.239
0.9	1.158	1.048	0.302	0.273
→1.0	→1.189	→1.189	→0.310	→0.310

Table 5. Stress intensity factors and crack opening displacements for an external edge crack in a thick-walled cylinder subjected to axial tension and pure bending. ($\ell/h=0.1$, $h=b-a$, $\sigma_0=P_\infty/[\pi(b^2-a^2)]$, $\sigma_1=4Mb/[\pi(b^4-a^4)]$).

$\frac{a}{b}$	$\frac{k(c)}{\sigma_0\sqrt{\ell}}$	$\frac{k(c)}{\sigma_1\sqrt{\ell}\cos\theta}$	$\frac{\mu}{1-\nu}\frac{\delta(d)}{h\,\sigma_0}$	$\frac{\mu}{1-\nu}\frac{\delta(d)}{h\sigma_1\cos\theta}$
0	1.181	1.166	0.302	0.308
0.1	1.176	1.159	0.302	0.306
0.2	1.172	1.153	0.302	0.304
0.3	1.170	1.149	0.302	0.303
0.4	1.168	1.147	0.302	0.302
0.5	1.167	1.147	0.302	0.301
0.6	1.167	1.149	0.303	0.301
0.7	1.168	1.152	0.303	0.302
0.8	1.169	1.158	0.304	0.303
0.9	1.173	1.166	0.306	0.305
→1.0	→1.189	→1.189	→0.310	→0.310

Table 6. Stress intensity factors and crack opening displacements for an internal edge crack in a thick-walled cylinder subjected to axial tension and pure bending. ($\ell/h=0.2$, $h=b-a$, $\sigma_0=P_\infty/[\pi(b^2-a^2)]$, $\sigma_1=4Mb/[\pi(b^4-a^4)]$).

$\frac{a}{b}$	$\frac{k(d)}{\sigma_0\sqrt{\ell}}$	$\frac{k(d)}{\sigma_1\sqrt{\ell}\cos\theta}$	$\frac{\mu}{1-\nu}\frac{\delta(c)}{h\,\sigma_0}$	$\frac{\mu}{1-\nu}\frac{\delta(c)}{h\sigma_1\cos}$
0	0.644	0.085	0.258	0
0.1	0.775	0.153	0.373	0.036
0.2	0.869	0.241	0.441	0.089
0.3	0.942	0.342	0.488	0.148
0.4	1.003	0.452	0.524	0.212
0.5	1.055	0.571	0.555	0.280
0.6	1.104	0.699	0.582	0.353
0.7	1.150	0.833	0.608	0.429
0.8	1.198	0.978	0.635	0.511
0.9	1.253	1.139	0.666	0.602
→1.0	→1.367	→1.367	→0.732	→0.732

Table 7. Stress intensity factors and crack opening displacements for an external edge crack in a thick-walled cylinder subjected to axial tension and pure bending. ($\ell/h=0.2$, $h=b-a$, $\sigma_0=P_\infty/[\pi(b^2-a^2)]$, $\sigma_1=4Mb/[\pi(b^4-a^4)]$).

$\frac{a}{b}$	$\frac{k(c)}{\sigma_0\sqrt{\ell}}$	$\frac{k(c)}{\sigma_1\sqrt{\ell}\cos\theta}$	$\frac{\mu}{1-\nu}\frac{\delta(d)}{h\,\sigma_0}$	$\frac{\mu}{1-\nu}\frac{\delta(d)}{h\sigma_1\cos\theta}$
0	1.260	1.314	0.625	0.705
0.1	1.244	1.279	0.622	0.685
0.2	1.235	1.253	0.623	0.669
0.3	1.231	1.234	0.626	0.658
0.4	1.230	1.222	0.630	0.651
0.5	1.232	1.217	0.635	0.647
0.6	1.238	1.218	0.643	0.648
0.7	1.247	1.226	0.652	0.652
0.8	1.261	1.243	0.663	0.661
0.9	1.285	1.274	0.680	0.677
→1.0	→1.367	→1.367	→0.732	→0.732

Table 8. Stress intensity factors and crack opening displacements for an internal edge crack in a thick-walled cylinder subjected to axial tension and pure bending. ($\ell/h=0.3$, $h=b-a$, $\sigma_0=P_\infty/[\pi(b^2-a^2)]$, $\sigma_1=4Mb/[\pi(b^4-a^4)]$).

$\frac{a}{b}$	$\frac{k(d)}{\sigma_0\sqrt{\ell}}$	$\frac{k(d)}{\sigma_1\sqrt{\ell}\cos\theta}$	$\frac{\mu}{1-\nu}\frac{\delta(c)}{h\,\sigma_0}$	$\frac{\mu}{1-\nu}\frac{\delta(c)}{h\sigma_1\cos\theta}$
0	0.651	0.127	0.390	0
0.1	0.753	0.188	0.526	0.050
0.2	0.840	0.266	0.626	0.123
0.3	0.918	0.359	0.707	0.210
0.4	0.991	0.466	0.776	0.308
0.5	1.060	0.587	0.841	0.419
0.6	1.130	0.724	0.906	0.543
0.7	1.203	0.876	0.973	0.681
0.8	1.286	1.053	1.050	0.841
0.9	1.392	1.267	1.150	1.038
→1.0	→1.660	→1.660	→1.410	→1.410

Table 9. Stress intensity factors and crack opening displacements for an external edge crack in a thick-walled cylinder subjected to axial tension and pure bending. ($\ell/h=0.3$, $h=b-a$, $\sigma_0=P_\infty/[\pi(b^2-a^2)]$, $\sigma_1=4Mb/[\pi(b^4-a^4)]$).

$\frac{a}{b}$	$\frac{k(c)}{\sigma_0\sqrt{\ell}}$	$\frac{k(c)}{\sigma_1\sqrt{\ell}\cos\theta}$	$\frac{\mu}{1-\nu}\frac{\delta(d)}{h\,\sigma_0}$	$\frac{\mu}{1-\nu}\frac{\delta(d)}{h\sigma_1\cos\theta}$
0	1.388	1.592	0.987	1.307
0.1	1.350	1.450	0.976	1.225
0.2	1.328	1.431	0.975	1.165
0.3	1.316	1.381	0.983	1.122
0.4	1.313	1.347	0.996	1.093
0.5	1.317	1.327	1.015	1.078
0.6	1.329	1.323	1.040	1.077
0.7	1.350	1.334	1.073	1.089
0.8	1.384	1.365	1.117	1.120
0.9	1.442	1.428	1.185	1.181
→1.0	→1.660	→1.660	→1.410	→1.410

Table 10. Stress intensity factors and crack opening displacements for an internal edge crack in a thick-walled cylinder subjected to axial tension and pure bending. ($\ell/h=0.4$, $h=b-a$, $\sigma_0=P_\infty/[\pi(b^2-a^2)]$, $\sigma_1=4Mb/[\pi(b^4-a^4)]$).

$\frac{a}{b}$	$\frac{k(d)}{\sigma_0\sqrt{\ell}}$	$\frac{k(d)}{\sigma_1\sqrt{\ell}\cos\theta}$	$\frac{\mu}{1-\nu}\frac{\delta(c)}{h\,\sigma_0}$	$\frac{\mu}{1-\nu}\frac{\delta(c)}{h\sigma_1\cos\theta}$
0	0.665	0.171	0.531	0
0.1	0.754	0.226	0.686	0.062
0.2	0.838	0.296	0.817	0.155
0.3	0.920	0.383	0.935	0.269
0.4	1.001	0.487	1.046	0.404
0.5	1.085	0.611	1.158	0.563
0.6	1.174	0.757	1.277	0.752
0.7	1.275	0.928	1.412	0.973
0.8	1.397	1.141	1.580	1.254
0.9	1.568	1.426	1.821	1.638
→1.0	→2.112	→2.112	→2.614	→2.614

Table 11. Stress intensity factors and crack opening displacements for an external edge crack in a thick-walled cylinder subjected to axial tension and pure bending. ($\ell/h=0.4$, $h=b-a$, $\sigma_0=P_\infty([\pi(b^2-a^2)]$, $\sigma_1=4Mb/[\pi(b^4-a^4)]$).

$\frac{a}{b}$	$\frac{k(c)}{\sigma_0\sqrt{\ell}}$	$\frac{k(c)}{\sigma_1\sqrt{\ell}\cos\theta}$	$\frac{\mu}{1-\nu}\frac{\delta(d)}{h\,\sigma_0}$	$\frac{\mu}{1-\nu}\frac{\delta(d)}{h\sigma_1\cos\theta}$
0	1.593	2.077	1.422	2.337
0.1	1.513	1.865	1.388	2.078
0.2	1.465	1.715	1.381	1.899
0.3	1.437	1.606	1.392	1.774
0.4	1.425	1.531	1.419	1.692
0.5	1.427	1.486	1.459	1.646
0.6	1.443	1.467	1.516	1.633
0.7	1.475	1.476	1.594	1.658
0.8	1.533	1.520	1.706	1.730
0.9	1.641	1.626	1.891	1.890
→1.0	→2.112	→2.112	→2.614	→2.614

Table 12. Stress intensity factors and crack opening displacements for an internal edge crack in a thick-walled cylinder subjected to axial tension and pure bending. ($\ell/h=0.5$, $h=b-a$, $\sigma_0=P_\infty/[\pi(b^2-a^2)]$, $\sigma_1=4Mb/[\pi(b^4-a^4)]$).

$\frac{a}{b}$	$\frac{k(d)}{\sigma_0\sqrt{\ell}}$	$\frac{k(d)}{\sigma_1\sqrt{\ell}\cos\theta}$	$\frac{\mu}{1-\nu}\frac{\delta(c)}{h\,\sigma_0}$	$\frac{\mu}{1-\nu}\frac{\delta(c)}{h\sigma_1\cos\theta}$
0	0.691	0.217	0.689	0
0.1	0.775	0.267	0.864	0.074
0.2	0.859	0.333	1.029	0.187
0.3	0.945	0.415	1.189	0.329
0.4	1.035	0.517	1.351	0.503
0.5	1.131	0.643	1.523	0.718
0.6	1.239	0.799	1.718	0.985
0.7	1.366	0.989	1.954	1.318
0.8	1.529	1.243	2.267	1.775
0.9	1.779	1.612	2.765	2.472
→1.0	→2.826	→2.826	→4.950	→4.950

Table 13. Stress intensity factors and crack opening displacements for an external edge crack in a thick-walled cylinder subjected to axial tension and pure bending. ($\ell/h=0.5$, $h=b-a$, $\sigma_0=P_\infty/[\pi(b^2-a^2)]$, $\sigma_1=4Mb/[\pi(b^4-a^4)]$).

$\frac{a}{b}$	$\frac{k(c)}{\sigma_0\sqrt{\ell}}$	$\frac{k(c)}{\sigma_1\sqrt{\ell}\cos\theta}$	$\frac{\mu}{1-\nu}\frac{\delta(d)}{h\,\sigma_0}$	$\frac{\mu}{1-\nu}\frac{\delta(d)}{h\sigma_1\cos\theta}$
0	1.922	2.929	1.989	4.291
0.1	1.762	2.468	1.901	3.548
0.2	1.667	2.163	1.873	3.076
0.3	1.610	1.946	1.884	2.753
0.4	1.580	1.780	1.924	2.546
0.5	1.572	1.707	1.994	2.426
0.6	1.586	1.660	2.097	2.382
0.7	1.627	1.658	2.248	2.417
0.8	1.709	1.712	2.478	2.558
0.9	1.878	1.867	2.888	2.904
→1.0	→2.826	→2.826	→4.950	→4.950

Table 14. Stress intensity factors and crack opening displacements for an internal edge crack in a thick-walled cylinder subjected to axial tension and pure bending. ($\ell/h=0.6$, $h=b-a$, $\sigma_0=P_\infty/[\pi(b^2-a^2)]$, $\sigma_1=4Mb/[\pi(b^4-a^4)]$).

$\frac{a}{b}$	$\frac{k(d)}{\sigma_0\sqrt{\ell}}$	$\frac{k(d)}{\sigma_1\sqrt{\ell}\cos\theta}$	$\frac{\mu}{1-\nu}\frac{\delta(c)}{h\,\sigma_0}$	$\frac{\mu}{1-\nu}\frac{\delta(c)}{h\sigma_1\cos\theta}$
0	0.736	0.265	0.877	0
0.1	0.820	0.314	1.077	0.087
0.2	0.908	0.378	1.283	0.222
0.3	1.000	0.459	1.493	0.393
0.4	1.099	0.561	1.716	0.611
0.5	1.208	0.691	1.966	0.890
0.6	1.333	0.856	2.261	1.253
0.7	1.484	1.066	2.636	1.729
0.8	1.688	1.359	3.166	2.431
0.9	2.025	1.824	4.091	3.623
→1.0	→4.035	→4.035	→9.965	→9.965

Table 15. Stress intensity factors and crack opening displacements for an external edge crack in a thick-walled cylinder subjected to axial tension and pure bending, ($\ell/h=0.6$, $h=b-a$, $\sigma_0=P_\infty/[\pi(b^2-a^2)]$, $\sigma_1=4Mb/[\pi(b^4-a^4)]$).

$\frac{a}{b}$	$\frac{k(c)}{\sigma_0\sqrt{\ell}}$	$\frac{k(c)}{\sigma_1\sqrt{\ell}\cos\theta}$	$\frac{\mu}{1-\nu}\frac{\delta(d)}{h\,\sigma_0}$	$\frac{\mu}{1-\nu}\frac{\delta(d)}{h\sigma_1\cos\theta}$
0	2.478	4.579	2.798	8.542
0.1	2.159	3.527	2.589	6.365
0.2	1.977	2.880	2.510	5.095
0.3	1.866	2.460	2.506	4.307
0.4	1.802	2.194	2.557	3.833
0.5	1.773	2.021	2.661	3.550
0.6	1.776	1.923	2.826	3.424
0.7	1.818	1.895	3.080	3.455
0.8	1.918	1.949	3.491	3.692
0.9	2.153	2.155	4.289	4.354
→1.0	→4.035	→4.035	→9.965	→9.965

Table 16. The effect of Poisson's ratio on stress intensity factors and $\delta(c)$ when loading is uniform tension ($a/b=0.5$, $\ell/h=0.3$, $\sigma_0=P_\infty/[\pi(b^2-a^2)]$, $h=b-a$).

	$\nu=0$	$\nu=0.1$	$\nu=0.2$	$\nu=0.3$	$\nu=0.4$	$\nu=0.5$
$\frac{k(d)}{\sigma_0\sqrt{\ell}}$	1.048	1.051	1.055	1.060	1.067	1.076
$\frac{\mu}{1-\nu}\frac{\delta(c)}{h\,\sigma_0}$	0.814	0.821	0.831	0.841	0.854	0.870

Table 17. The effect of Poisson's ratio on stress intensity factors and $\delta(c)$ when loading is pure bending ($a/b=0.5$, $\ell/h=0.3$, $\sigma_1=4Mb/[\pi(b^4-a^4)]$, $h=b-a$).

	$\nu=0$	$\nu=0.1$	$\nu=0.2$	$\nu=0.3$	$\nu=0.4$	$\nu=0.5$
$\frac{k(d)}{\sigma_1\sqrt{\ell}\cos\theta}$	0.574	0.577	0.582	0.587	0.594	0.602
$\frac{\mu}{1-\nu}\frac{\delta(c)}{h\sigma_1\cos\theta}$	0.395	0.402	0.410	0.419	0.430	0.443

APPENDIX A

The functions $C_{in}(s)$ which appear in (28) $(m_{ij}(s)) = M(s) = F^{-1}(s)$, $F(s) = (f_{ij}(s))$, $(i,j) = 1,\ldots,6$. The coefficients f_{ij} of the matrix F are

$$f_{i1} = rs\, I_n(sr) - (2-2\nu+n)\, I_{n+1}(sr) \tag{A-1}$$

$$f_{i2} = -[rs\, K_n(sr) + (2-2\nu+n)\, K_{n+1}(sr)] \tag{A-2}$$

$$f_{i3} = s\, I_{n+1}(sr) + \frac{n}{r} I_n(sr) \tag{A-3}$$

$$f_{i4} = \frac{n}{r} K_n(sr) - s\, K_{n+1}(sr) \tag{A-4}$$

$$f_{i5} = -\frac{n}{r} I_n(sr) \tag{A-5}$$

$$f_{i6} = -\frac{n}{r} K_n(sr)\ ,\ i = 1,2\quad , \tag{A-6}$$

for $i = 1$, $r = a$ and for $i = 2$, $r = b$.

$$f_{i1} = -\frac{(n+1)}{r}(4-4\nu+n)\, I_{n+1}(sr) + (2-2\nu+n)s\, I_n(sr) \tag{A-7}$$

$$f_{i2} = -\frac{(n+1)}{r}(4-4\nu+n)K_{n+1}(sr) - (2-2\nu+n)s\, K_n(sr) \tag{A-8}$$

$$f_{i3} = \frac{sn}{r} I_{n+1}(sr) + \frac{n}{r^2}(n-1)\, I_n(sr) \tag{A-9}$$

$$f_{i4} = -\frac{sn}{r} K_{n+1}(sr) + \frac{n}{r^2}(n-1)\, K_n(sr) \tag{A-10}$$

$$f_{i5} = -\left(\frac{2n}{r^2}(n-1)+s^2\right)I_n(sr) + \frac{2s}{r} I_{n+1}(sr) \tag{A-11}$$

$$f_{i6} = -\left(\frac{2n}{r^2}(n-1)+s^2\right)K_n(sr) - \frac{2s}{r} K_{n+1}(sr) \tag{A-12}$$

for $i = 3,4$; when $i = 3$, $r = a$ and when $i = 4$, $r = b$.

$$f_{i1} = (3-2\nu)s\, I_n(sr) - \left[\frac{(n+1)}{r}(4-4\nu+n) + rs^2\right]I_{n+1}(sr) \tag{A-13}$$

$$f_{i2} = -\{(3-2\nu)s\, K_n(sr) + \left[\frac{(n+1)}{r}(4-4\nu+n) + rs^2\right]K_{n+1}(sr)\} \tag{A-14}$$

$$f_{i3} = -\{\left[\frac{n(n-1)}{r^2} + s^2\right]I_n(sr) - \frac{s}{r} I_{n+1}(sr)\} \tag{A-15}$$

$$f_{i4} = -\{\left[\frac{n(n-1)}{r^2} + s^2\right]K_n(sr) + \frac{s}{r} K_{n+1}(sr)\} \tag{A-16}$$

$$f_{i5} = \frac{2n}{r}\left[\frac{(n-1)}{r} I_n(sr) + s\, I_{n+1}(sr)\right] \tag{A-17}$$

$$f_{i6} = \frac{2n}{r}\left[\frac{(n-1)}{r} K_n(sr) - s\, K_{n+1}(sr)\right] \tag{A-18}$$

for $i = 5,6$; when $i = 5$, $r = a$ and when $i = 6$, $r = b$.

The terms $G_j(s,t)$ in (28) are obtained by evaluating the Bessel integrals which result from the substitution of (27) into equations (8), (11), (12), (14) and (21)-(24). These definite Bessel integrals are evaluated by differentiating a related integral given in [17], that is, by using

$$\int_0^\infty \alpha^{\nu-\mu+2n+1}\,(s^2+\alpha^2)^{-1} J_\mu(a\alpha)J_\nu(t\alpha)\,d\alpha = (-1)^n s^{\nu-\mu+2n} I_\mu(as)K_\nu(ts)$$

$$a > 0,\ \mathrm{Re}\ s > 0,\ a < t < \infty,$$

$$\mathrm{Re}\ \mu - 2n+1 > \mathrm{Re}\ \nu > -n-1\ ,\ n = \text{integer}. \tag{A-19}$$

Taking the derivative with respect to s on both sides, the integral becomes,

$$\int_0^\infty \alpha^{\nu-\mu+2n+1}(s^2+\alpha^2)^{-2}J_\mu(a\alpha)J_\nu(t\alpha)d\alpha = \frac{(-1)^n}{-2}\cdot\{(\nu-\mu+2n)\ *$$

$$* s^{\nu-\mu+2n-2}I_\mu(as)K_\nu(ts) + s^{\nu-\mu+2n-1}[a\ I_{\mu+1}(sa) + \frac{\mu}{s}\ I_\mu(sa)]*$$

$$* K_\nu(ts) + s^{\nu-\mu+2n-1}\ I_\mu(as)[\frac{\nu}{s}\ K_\nu(st) - t\ K_{\nu+1}(st)]\}$$

$$a > 0\ ,\text{Re}\ s > 0,\ a < t < \infty, \qquad \text{(A-20)}$$

$$\text{Re}\ \mu-2n+4 > \text{Re}\ \nu > -n-1$$

Thus, the terms $G_j(s,t)$ $(j=1,6)$ are expressed as:

$$G_1(s,t) = K_n(st)\{\frac{2n(n+1)}{a}\ I_n(as) + (4+3n)s\ I_{n+1}(as)$$

$$+ s^2\ a\ I_{n+2}(as)\} - t\ K_{n+1}(st)\ \{\frac{ns}{a}\ I_n(as) + s^2\ I_{n+1}(as)\} \qquad \text{(A-21)}$$

$$G_2(s,t) = I_n(st)\{\frac{2n(n+1)}{b}\ K_n(bs) - (4+3n)s\ K_{n+1}(bs)$$

$$+ s^2\ b\ K_{n+2}(bs)\} + t\ I_{n+1}(st)\ \{\frac{ns}{b}\ K_n(bs) - s^2K_{n+1}(bs)\} \qquad \text{(A-22)}$$

$$G_3(s,t) = \frac{n}{a}\ \{K_n(st)[\frac{2(n-1)(\nu+n)}{a}\ I_n(as) + s(2\nu+3n+1)I_{n+1}(as)$$

$$+ s^2a\ I_{n+2}(as)] - t\ K_{n+1}(st)[\frac{s(n-1)}{a}\ I_n(as) + s^2I_{n+1}(as)]\} \qquad \text{(A-23)}$$

$$G_4(s,t) = \frac{n}{b}\{I_n(st)[\frac{2(n-1)(\nu+n)}{b} K_n(bs) - s(2\nu+3n+1)K_{n+1}(bs)$$

$$+ s^2 b\, K_{n+2}(bs)] + t\, I_{n+1}(st)[\frac{s(n-1)}{b} K_n(bs) - s^2 K_{n+1}(bs)]\} \qquad \text{(A-24)}$$

$$G_5(s,t) = K_n(st)\{-[\frac{2n(n-1)(n+\nu)}{a^2} + 2(n+1)s^2]I_n(sa)$$

$$+ [\frac{s}{a}(-n^2+3n+2(\nu+1))-s^3 a]I_{n+1}(sa) + s^2 I_{n+2}(sa)\}$$

$$-t\, K_{n+1}(st)\{-[\frac{n(n-1)}{a^2}+s^2]s\, I_n(as) + \frac{s^2}{a} I_{n+1}(as)\} \qquad \text{(A-25)}$$

$$G_6(s,t) = I_n(st)\{-[\frac{2n(n-1)(n+\nu)}{b^2} + 2(n+1)s^2]K_n(bs)$$

$$+ [\frac{s}{b}(n^2-3n-2(\nu+1)) + s^3 b]K_{n+1}(bs) + s^2 K_{n+2}(bs)\}$$

$$+ t\, I_{n+1}(st)\{-[\frac{n(n-1)}{b^2} + s^2]s\, K_n(bs) - \frac{s^2}{b} K_{n+1}(bs)\} \qquad \text{(A-26)}$$

APPENDIX B

The functions $v_j(s,t)$ which appear in (30)

$$v_j = \gamma_{jK} Q_K \quad \text{for} \quad j = 1,3,5 \ , \quad K = 1,2 \tag{B-1}$$

$$v_j = \gamma_{jK} Q_{K+2} \quad \text{for} \quad j = 2,4,6 \ , \quad K = 1,2 \ . \tag{B-2}$$

For example,

$$v_1 = \gamma_{11}Q_1 + \gamma_{12}Q_2$$

$$v_2 = \gamma_{21}Q_3 + \gamma_{22}Q_4$$

$$v_3 = \gamma_{31}Q_1 + \gamma_{32}Q_2 \ , \text{ etc.}$$

$$\gamma_{11} = \frac{2n(n+1)}{a} I_n(as) + (4+3n)s\, I_{n+1}(as) + s^2 a\, I_{n+2}(as) \tag{B-3}$$

$$\gamma_{12} = \frac{ns}{a} I_n(as) + s^2 I_{n+1}(as) \tag{B-4}$$

$$\gamma_{21} = \frac{2n(n+1)}{b} K_n(bs) - (4+3n)s\, K_{n+1}(bs) + s^2 b\, K_{n+2}(bs) \tag{B-5}$$

$$\gamma_{22} = \frac{ns}{b} K_n(bs) - s^2 K_{n+1}(bs) \tag{B-6}$$

$$\gamma_{31} = \frac{n}{a}\left[\frac{2(n-1)(\nu+n)}{a} I_n(as) + s(2\nu+3n+1) I_{n+1}(as) + s^2 a\, I_{n+2}(as)\right] \tag{B-7}$$

$$\gamma_{32} = \frac{n}{a}\left[\frac{s(n-1)}{a} I_n(as) + s^2 I_{n+1}(as)\right] \tag{B-8}$$

$$\gamma_{41} = \frac{n}{b}\left[\frac{2(n-1)(\nu+n)}{b} K_n(bs) - s(2\nu+3n+1) K_{n+1}(bs) + s^2 b\, K_{n+2}(bs)\right] \tag{B-9}$$

$$\gamma_{42} = \frac{n}{b}\left[\frac{s(n-1)}{b} K_n(bs) - s^2 K_{n+1}(bs)\right] \tag{B-10}$$

$$\gamma_{51} = -\left[\frac{2n(n-1)(n+\nu)}{a^2} + 2(n+1)s^2\right] I_n(sa) + \left[\frac{s}{a}\left(-n^2+3n+2(\nu+1)\right)\right.$$

$$\left. - s^3 a\right] I_{n+1}(sa) + s^2 I_{n+2}(sa) \tag{B-11}$$

$$\gamma_{52} = -\left[\frac{n(n-1)}{a^2} + s^2\right] s\, I_n(as) + \frac{s^2}{a} I_{n+1}(as) \tag{B-12}$$

$$\gamma_{61} = -\left[\frac{2n(n-1)(n+\nu)}{b^2} + 2(n+1)s^2\right] K_n(bs) + \left[\frac{s}{b}\left(n^2-3n-2(\nu+1)\right)\right.$$

$$\left. + s^3 b\right] K_{n+1}(bs) + s^2 K_{n+2}(bs) \tag{B-13}$$

$$\gamma_{62} = -\left[\frac{n(n-1)}{b^2} + s^2\right] s\, K_n(bs) - \frac{s^2}{b} K_{n+1}(bs) \tag{B-14}$$

The terms in (B-1) and (B-2) denoted by Q_K are defined as,

$$Q_1(s,t) = -\frac{i}{s}\left[nt\, K_n(st) S_{o,n-1}(ist) - it\, K_{n-1}(st) S_{1,n}(ist)\right] \tag{B-15}$$

$$Q_2(s,t) = \frac{1}{s^2}\left[(n+2)t\, K_{n+1}(st) S_{1,n}(ist) - it\, K_n(st) S_{2,n+1}(ist)\right] \tag{B-16}$$

$$Q_3(s,t) = -\frac{i}{s}\left[nt\, I_n(st) S_{o,n-1}(ist) + it\, I_{n-1}(st) S_{1,n}(ist)\right] \tag{B-17}$$

$$Q_4(s,t) = -\frac{1}{s^2}\left[(n+2)t\, I_{n+1}(st) S_{1,n}(ist) + it\, I_n(st) S_{2,n+1}(ist)\right]. \tag{B-18}$$

The Lommel functions of imaginary argument which are encountered in Q_K are not in a form which is convenient for numerical

computation, but with the aid of certain identities involving the Struve function Q_K may be expressed in terms of real functions with real arguments. The terms Q_K K=1,...,4 for five harmonics n=0,...,4 are given below.

n=0

$$Q_1(s,t) = \frac{-t}{s} K_1(st) \tag{B-19}$$

$$Q_2(s,t) = \frac{2t}{s^2} K_1(st) + \frac{t^2}{s} K_0(st) \tag{B-20}$$

$$Q_3(s,t) = \frac{t}{s} I_1(st) \tag{B-21}$$

$$Q_4(s,t) = -\frac{2t}{s^2} I_1(st) + \frac{t^2}{s} I_0(st) \tag{B-22}$$

let: $$u_0(z) = z\int_0^1 e^{-zp} (1-p^2)^{-1/2}\, dp \tag{B-23}$$

$$u_1(z) = \int_0^1 e^{-zp} (1-p^2)^{1/2}\, dp \tag{B-24}$$

$$u_2(z) = z^2 \int_0^1 e^{-zp} (1-p^2)^{3/2}\, dp, \tag{B-25}$$

then for n=1:

$$Q_1(s,t) = \frac{-t}{s} [K_1(st)u_0(st) + K_0(st)u_1(st)] \tag{B-26}$$

$$Q_2(s,t) = \frac{t}{s^2} [3K_2(st)u_1(st) + K_1(st)u_2(st)] \tag{B-27}$$

$$Q_3(s,t) = \frac{t}{s}\,[I_0(st)u_1(st) - I_1(st)u_0(st)] \qquad \text{(B-28)}$$

$$Q_4(s,t) = \frac{-t}{s^2}\,[3I_2(st)u_1(st) - I_1(st)u_2(st)] \qquad \text{(B-29)}$$

n=2

$$Q_1(s,t) = \frac{-2}{s^2}\,K_2(st) - \frac{t}{s}\,[1 - \frac{4}{(st)^2}]K_1(st) \qquad \text{(B-30)}$$

$$Q_2(s,t) = \frac{4t}{s^2}\,[1 - \frac{4}{(st)^2}]K_3(st) + \frac{t}{s^2}\,[st - \frac{8}{st} + \frac{64}{(st)^3}]K_2(st) \qquad \text{(B-31)}$$

$$Q_3(s,t) = -\frac{2}{s^2}\,I_2(st) + \frac{t}{s}\,[1 - \frac{4}{(st)^2}]I_1(st) \qquad \text{(B-32)}$$

$$Q_4(s,t) = \frac{-4t}{s^2}\,[1 - \frac{4}{(st)^2}]I_3(st) + \frac{t}{s^2}\,[st - \frac{8}{st} + \frac{64}{(st)^3}]I_2(st) \qquad \text{(B-33)}$$

n=3

$$Q_1(s,t) = \frac{t}{s}\,\{K_3(st)[3u_0(st) - \frac{6}{st}\,u_1(st)] + K_2(st)[3u_1(st) - \frac{4}{st}\,u_2(st)]\} \qquad \text{(B-34)}$$

$$Q_2(s,t) = \frac{t}{s^2}\,\{K_4(st)[\frac{20}{st}\,u_2(st) - 15\,u_1(st)] + K_3(st)[st - 15\,u_0(st) + \frac{120}{st}\,u_1(st) - \frac{120}{(st)^2}\,u_2(st)]\} \qquad \text{(B-35)}$$

$$Q_3(s,t) = \frac{t}{s}\,\{I_3(st)[3\,u_0(st) - \frac{6}{st}\,u_1(st)] - I_2(st)[3u_1(st) - \frac{4}{st}\,u_2(st)]\} \qquad \text{(B-36)}$$

$$Q_4(s,t) = \frac{-t}{s^2}\,\{I_4(st)[\frac{20}{st}\,u_2(st) - 15u_1(st)] + I_3(st)[-st + 15u_0(st) - \frac{120}{st}\,u_1(st) + \frac{120}{(st)^2}\,u_2(st)]\} \qquad \text{(B-37)}$$

n=4

$$Q_1(s,t) = \frac{4t}{s}\left[-\frac{1}{st} + \frac{8}{(st)^3}\right]K_4(st) - \frac{t}{s}\left[1 - \frac{16}{(st)^2} + \frac{192}{(st)^4}\right]K_3(st) \qquad \text{(B-38)}$$

$$Q_2(s,t) = \frac{6t}{s^2}\left[1 - \frac{16}{(st)^2} + \frac{192}{(st)^4}\right]K_5(st) + \frac{t}{s^2}\left[st - \frac{24}{st} + \frac{576}{(st)^3} - \frac{9216}{(st)^5}\right]K_4(st) \qquad \text{(B-39)}$$

$$Q_3(s,t) = \frac{4t}{s}\left[-\frac{1}{st} + \frac{8}{(st)^3}\right]I_4(st) + \frac{t}{s}\left[1 - \frac{16}{(st)^2} + \frac{192}{(st)^4}\right]I_3(st) \qquad \text{(B-40)}$$

$$Q_4(s,t) = \frac{-6t}{s^2}\left[1 - \frac{16}{(st)^2} + \frac{192}{(st)^4}\right]I_5(st) + \frac{t}{s^2}\left[st - \frac{24}{st} + \frac{576}{(st)^3} - \frac{9216}{(st)^5}\right]I_4(st) \qquad \text{(B-41)}$$

APPENDIX C

Evaluation of Lommel's Functions

In the problem considered, Lommel's functions $S_{\mu,\nu}$ arise from the indefinite integrals of the form

$$\int z^{\mu} J_{\nu}(z)dz = (\mu+\nu-1)z\, J_{\nu}(z)S_{\mu-1,\nu-1}(z) - z\, J_{\nu-1}(z)S_{\mu,\nu}(z) \tag{C-1}$$

$$S_{\mu,\nu}(z) = z^{\mu-1}\left[1 - \frac{(\mu-1)^2-\nu^2}{z^2} + \frac{[(\mu-1)^2-\nu^2][(\mu-3)^2-\nu^2]}{z^4} - \ldots\right] \tag{C-2}$$

Referring to [12] it can be shown that the Lommel's functions of real argument may be expressed as

$$n = 0 \qquad S_{1,0}(z) = 1 \tag{C-3}$$

$$n = 1 \qquad \begin{cases} S_{0,0}(z) = \displaystyle\int_0^{\infty} (1+t^2)^{-1/2} e^{-zt}\, dt & \text{(C-4)} \\ S_{1,1}(z) = z\displaystyle\int_0^{\infty} (1+t^2)^{1/2} e^{-zt}\, dt & \text{(C-5)} \end{cases}$$

$$n = 2 \qquad \begin{cases} S_{0,1}(z) = z^{-1} & \text{(C-6)} \\ S_{1,2}(z) = 1 + 4z^{-2} & \text{(C-7)} \end{cases}$$

$$n=3 \quad \begin{cases} S_{0,2}(z) = 2z^{-1} S_{1,1}(z) - S_{0,0}(z) & \text{(C-8)} \\ S_{1,3}(z) = 4 + (24z^{-2}-3)S_{1,1}(z) - 12z^{-1}S_{0,0}(z) & \text{(C-9)} \end{cases}$$

$$n=4 \quad \begin{cases} S_{0,3}(z) = z^{-1} + 8z^{-3} & \text{(C-10)} \\ S_{1,4}(z) = 1 + 16z^{-2} + 192z^{-4} & \text{(C-11)} \end{cases}$$

$$n=5 \quad \begin{cases} S_{0,4}(z) = 8z^{-1} + (48z^{-3}-8z^{-1})S_{1,1}(z) + (1-24z^{-2})S_{0,0}(z) & \text{(C-12)} \\ S_{1,5}(z) = -4 + 320z^{-2} + (1920z^{-4}-360z^{-2}+5)S_{1,1}(z) \\ \qquad + (60z^{-1}-960z^{-3})S_{0,0}(z) & \text{(C-13)} \end{cases}$$

The details for evaluating $S_{\mu,\nu}$ asymptotically for small and large arguments may be found in [19].

APPENDIX D

Evaluation of the Integral in (32)

As noted in Section 2, to evaluate the integral in (32) it is necessary to analyze the integrand asymptotically. By using the asymptotic expansions for $J_n(z)$, $S_{\mu,\nu}(z)$, $S(x)$, and $C(x)$ as given by [12-14] and by evaluating the integral in $A<\alpha<\infty$ asymptotically, (32) may be expressed as

$$L_1(t,r) = \frac{-1}{\pi}\frac{1}{2r}\log\left[\frac{(t^{\frac{1}{2}}-r^{\frac{1}{2}})^2}{|t-r|}\right] - \frac{1}{\pi}\left[\frac{1}{t-r} - \frac{\cos A(t-r)}{t-r} - (-1)^n\frac{\sin A(t+r)}{t+r}\right] + \int_0^A \{\alpha t[nJ_n(\alpha t)S_{0,n-1}(\alpha t) - J_{n-1}(\alpha t)S_{1,n}(\alpha t)]J_n(\alpha r) - \frac{1}{\sqrt{2\pi r\alpha}}[C(\sqrt{\alpha t})(\sin(\alpha r)+(-1)^n\cos(\alpha r)) - S(\sqrt{\alpha t})(\cos(\alpha r)+(-1)^n\sin(\alpha r))]\}d\alpha + [A_1+A_2+A_3], \quad n=0,1,\ldots \tag{D-1}$$

where A is a "large" number and A_1, A_2, and A_3 are given by

$$A_1 = \frac{n}{\pi}\left(\frac{t}{r}\right)^{\frac{1}{2}}\{-Ci(A(t-r)) + (-1)^n[\frac{\pi}{2} - Si(A(t+r))] + [\frac{4n^2-1}{8}\frac{1}{tr} - \frac{(4n^2-1)(4n^2-9)}{128}(\frac{1}{t^2}+\frac{1}{r^2})] * [\frac{\cos A(t-r)}{2A^2} + (-1)^n\frac{\sin A(t+r)}{2A^2} - \frac{(t-r)}{2}\frac{\sin A(t-r)}{A} + (-1)^n\frac{(t+r)}{2}\frac{\cos A(t+r)}{A} + \frac{(t-r)^2}{2}Ci(A(t-r)) - (-1)^n\frac{(t+r)^2}{2}[\frac{\pi}{2} - Si(A(t+r))]] + \frac{4n^2-1}{8}(\frac{1}{r}-\frac{1}{t}) * [\frac{\sin A(t-r)}{A} + (-1)^n\frac{\cos A(t+r)}{A} - (t-r)Ci(A(t-r))$$

$$- (-1)^n(t+r)\left[\frac{\pi}{2} - \mathrm{Si}(A(t+r))\right]\Big]\Big\} \qquad \text{(D-2)}$$

$$A_2 = \frac{1}{\pi}\left(\frac{t}{r}\right)^{\frac{1}{2}}\Big\{\Big[-\frac{(4n^2-1)(4n^2-9)}{128}\,r^{-2}$$

$$-\frac{(4(n-1)^2-1)(4(n-1)^2-9)-64n^2}{128}\,t^{-2}\Big]\Big[\frac{\sin A(t-r)}{A}$$

$$-(t-r)\mathrm{Ci}(A(t-r)) - (-1)^n\frac{\cos A(t+r)}{A} + (-1)^n(t+r)\left(\frac{\pi}{2}\right.$$

$$\left.-\mathrm{Si}(A(t+r))\right)\Big] + \frac{4(n-1)^2-1}{8}\,t^{-1}\,[-\mathrm{Ci}(A(t-r))$$

$$+(-1)^n\left(\frac{\pi}{2} - \mathrm{Si}(A(t+r))\right)\Big] + \frac{4n^2-1}{8}\,r^{-1}\,[\mathrm{Ci}(A(t-r))$$

$$+(-1)^n\left(\frac{\pi}{2} - \mathrm{Si}(A(t+r))\right)\Big] + \frac{(4n^2-1)(4(n-1)^2-1)}{64}\,(rt)^{-1}*$$

$$*\Big[\frac{\sin A(t-r)}{A} - (t-r)\mathrm{Ci}(A(t-r)) + (-1)^n\frac{\cos A(t+r)}{A}$$

$$-(-1)^n(t+r)\left(\frac{\pi}{2} - \mathrm{Si}(A(t+r))\right)\Big]\Big\} \qquad \text{(D-3)}$$

$$A_3 = -\frac{1-(-1)^n}{2r}\left[C(\sqrt{Ar}) - S(\sqrt{Ar})\right] - \frac{1}{2\pi}\,(rt)^{-\frac{1}{2}}*$$

$$*\Big[(-1)^n\Big[\frac{\pi}{2} - \mathrm{Si}(A(t+r))\Big] - \mathrm{Ci}(A(t-r))\Big] - \frac{1}{4\pi}\,r^{-\frac{1}{2}}\,t^{-3/2}*$$

$$*\Big[-\frac{\sin A(t-r)}{A} + (t-r)\mathrm{Ci}(A(t-r)) + (-1)^n\frac{\cos A(t+r)}{A}$$

$$-(-1)^n\,(t+r)\left(\frac{\pi}{2} - \mathrm{Si}(A(t+r))\right)\Big]\,, \quad n = 0,1,2,\ldots, \qquad \text{(D-4)}$$

The definite integral in (D-1) is evaluated by using Gauss-Legendre quadrature with the upper limit A = 200.

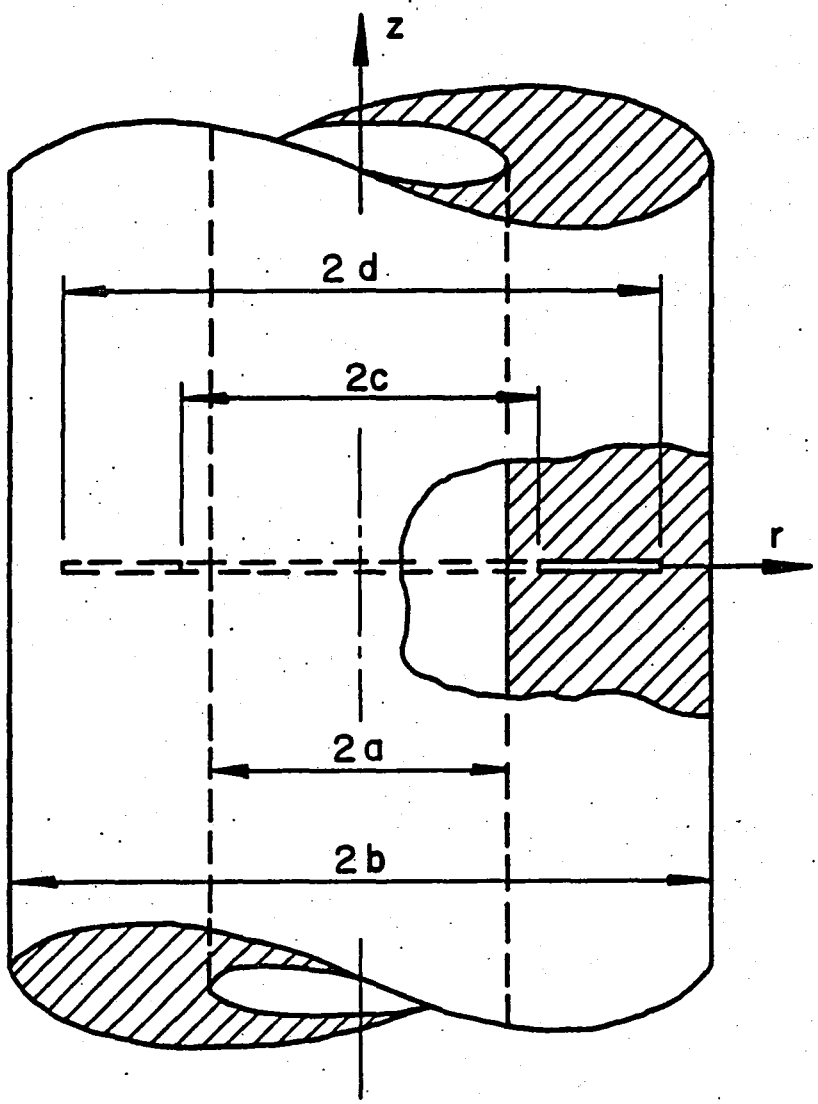

Fig. 1 Geometry of a thick-walled cylinder containing an axisymmetric circumferential crack.

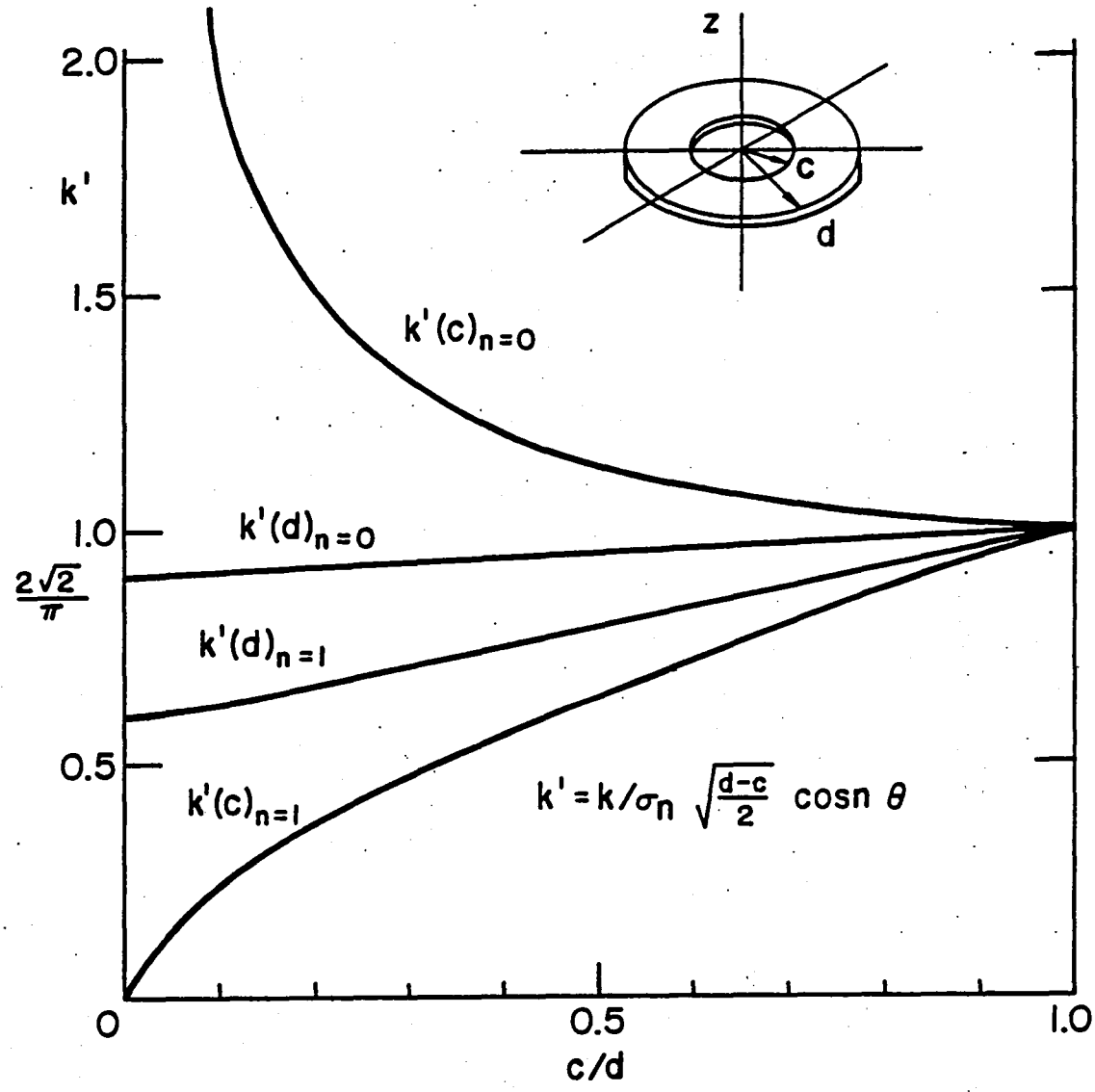

Fig. 2 Stress intensity factors for concentric ring shaped cracks in an infinite medium subjected to axial extension (n=0) and pure bending (n=1).

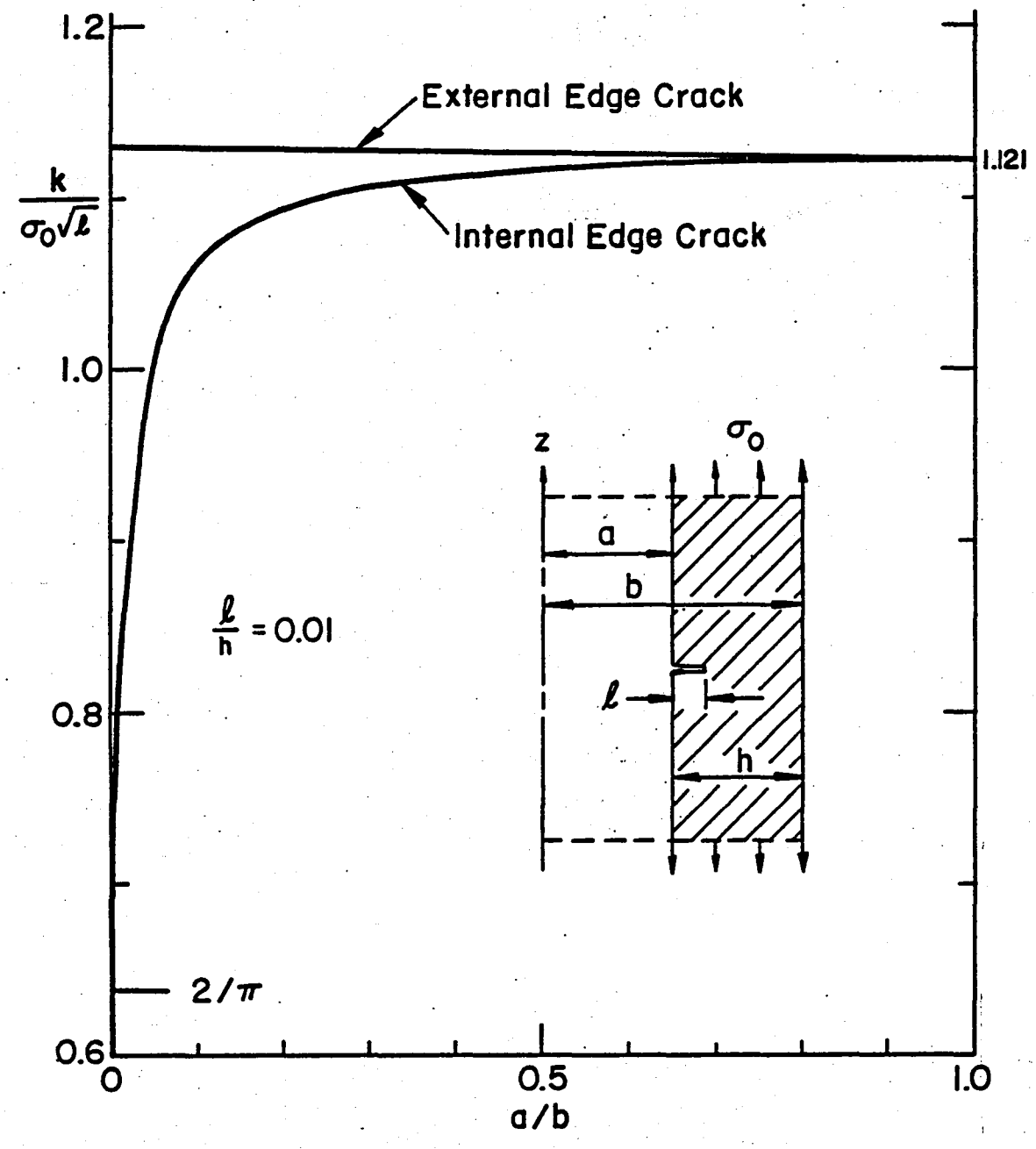

Fig. 3 Stress intensity factors for edge cracks in a thick-walled cylinder subjected to axial tension. $\ell/h = 0.01$.

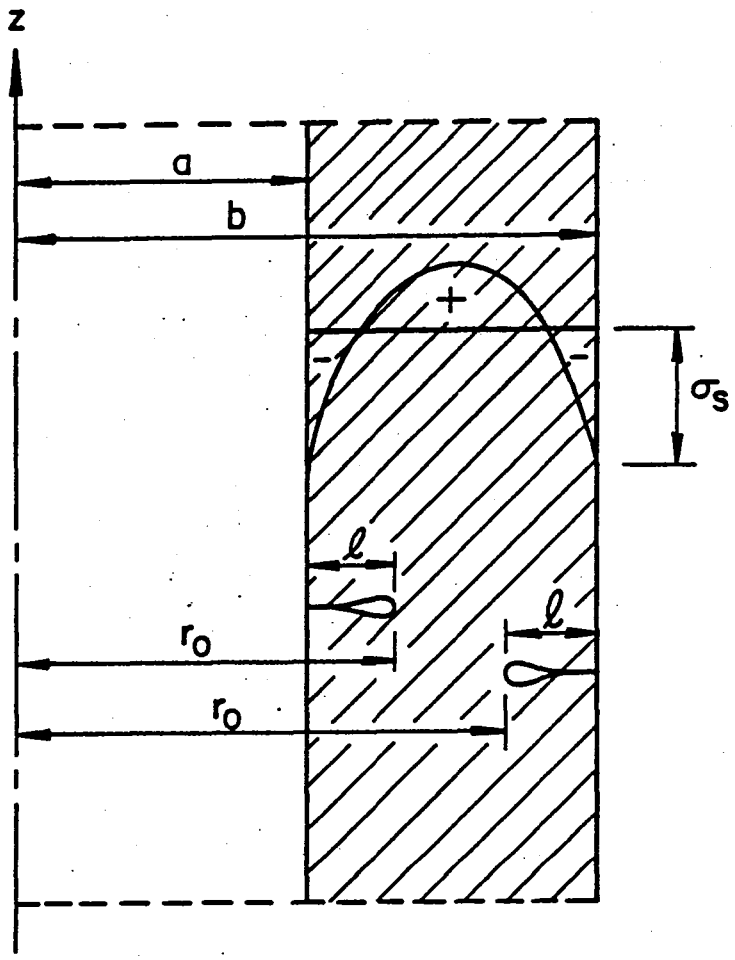

Fig. 4 Geometry of edge cracks in a cylinder wall subjected to residual stresses.

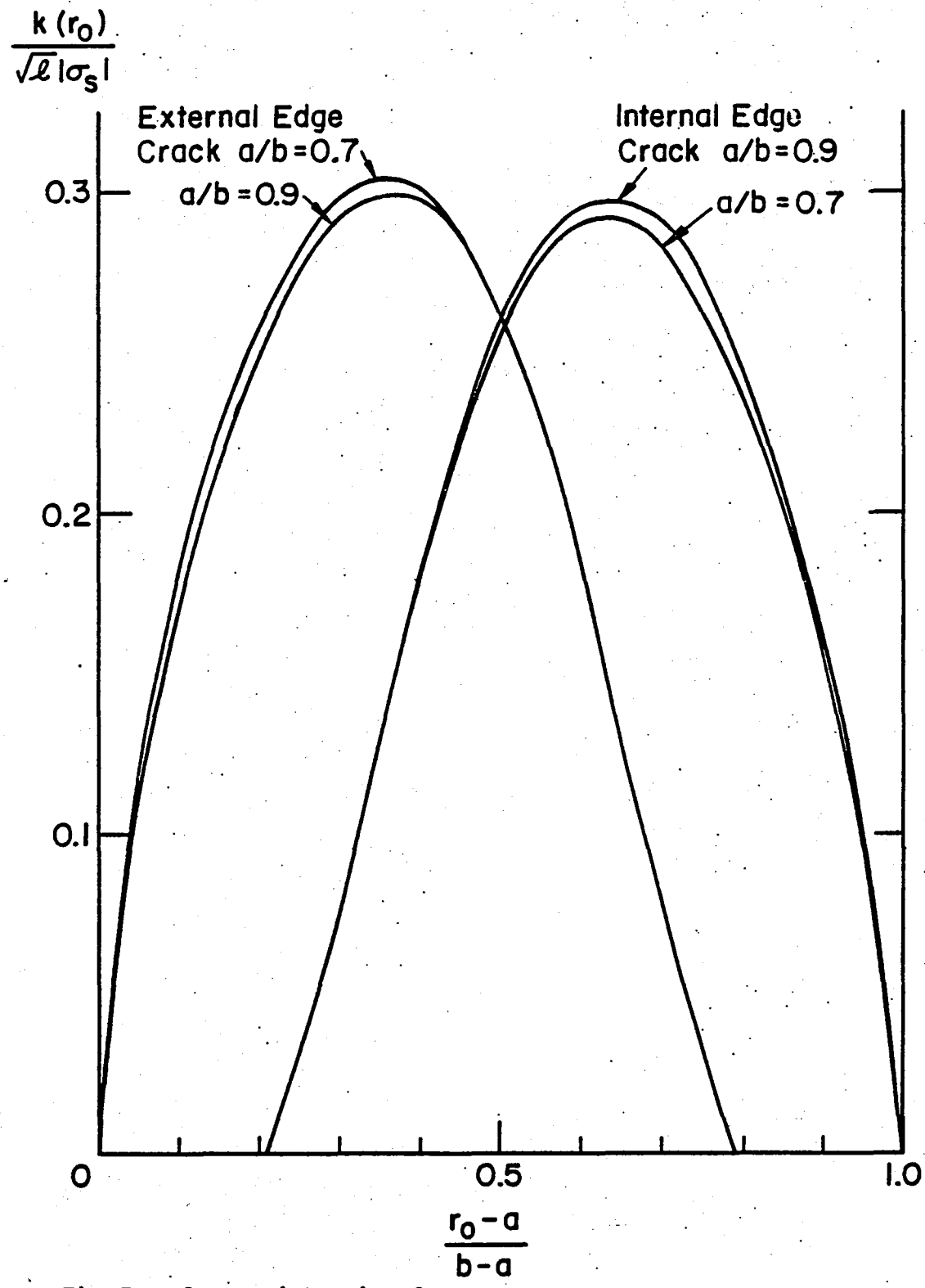

Fig. 5 Stress intensity factors for edge cracks in a hollow cylinder subjected to residual stresses. a/b = 0.9, a/b = 0.7.

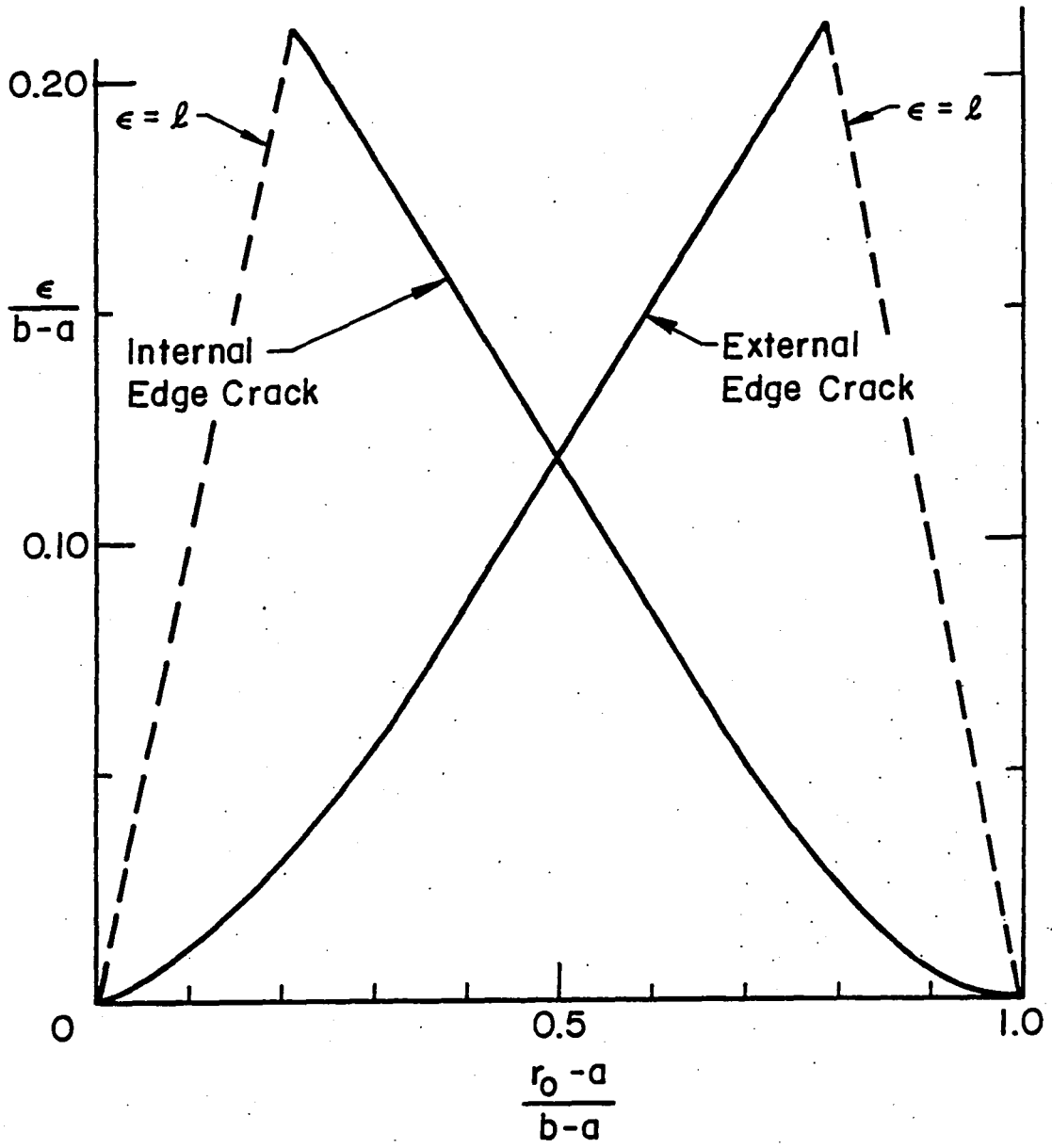

Fig. 6 Crack contact length ε for a hollow cylinder under residual stresses with either internal or external circumferential edge crack. a/b = 0.9.

1. Report No.	2. Government Accession No.	3. Recipient's Catalog No.
NASA CR-165988		

4. Title and Subtitle	5. Report Date
THE ELASTICITY PROBLEM FOR A THICK-WALLED CYLINDER CONTAINING A CIRCUMFERENTIAL CRACK	September 1982
	6. Performing Organization Code
7. Author(s)	8. Performing Organization Report No.
H. F. Nied and F. Erdogan	
	10. Work Unit No.
9. Performing Organization Name and Address	
Lehigh University Bethlehem, PA 18015	11. Contract or Grant No. NGR 39-007-011
	13. Type of Report and Period Covered Contractor Report
12. Sponsoring Agency Name and Address	
National Aeronautics and Space Administration Washington, DC 20546	14. Sponsoring Agency Code

15. Supplementary Notes

Langley technical monitor: Dr. John H. Crews, Jr.

16. Abstract

The elasticity problem for a long, hollow, circular cylinder containing an axisymmetric circumferential crack subjected to general nonaxisymmetric external loads is considered. The problem is formulated in terms of a system of singular integral equations with the Fourier coefficients of the derivative of the crack surface displacement as density functions. The stress-intensity factors and the crack-opening displacement are calculated for a cylinder under uniform tension, bending by end couples, and self-equilibrating residual stresses.

17. Key Words (Suggested by Author(s))		18. Distribution Statement
Hollow cylinder	Integral equations	Unclassified - Unlimited
Circumferential crack	Stress-intensity factor	
Tension		
Bending	Crack-opening displacement	Subject Category 39
Residual stress		

19. Security Classif. (of this report)	20. Security Classif. (of this page)	21. No. of Pages	22. Price*
Unclassified	Unclassified	45	A03

* For sale by the National Technical Information Service, Springfield, Virginia 22161

End of Document